J. Fluid Mech. (2005), *vol.* 522, *pp.* 383–394.
DOI: 10.1017/S0022112004002009 Printed in the United Kingdom

Pressure corrections for potential flow analysis of capillary instability of viscous fluids

By J. WANG[1], D. D. JOSEPH[1] AND T. FUNADA[2]

[1]Department of Aerospace Engineering and Mechanics, University of Minnesota, 110 Union St. SE, Minneapolis, MN 55455, USA

[2]Department of Digital Engineering, Numazu College of Technology, 3600 Ooka, Numazu, Shizuoka, 410-8501, Japan

(Received 16 March 2004 and in revised form 12 August 2004)

Funada & Joseph (*Intl J. Multiphase Flow*, vol. 28, 2002, p. 1459) analysed capillary instability assuming that the flow is irrotational but the fluids are viscous (viscous potential flow, VPF). They compared their results with the exact normal-mode solution of the linearized Navier–Stokes equations (fully viscous flow, FVF) and with the irrotational flow of inviscid fluids (inviscid potential flow, IPF). They showed that the growth rates computed by VPF are close to the exact solution when Reynolds number is larger than $O(10)$ and are always more accurate than those computed using IPF. Recently, Joseph & Wang (*J. Fluid Mech.*, vol. 505, 2004, p. 365) presented a method for computing a viscous correction of the irrotational pressure induced by the discrepancy between non-zero irrotational shear stress and the zero-shear-stress boundary condition at a free surface. The irrotational flow with a corrected pressure is called the viscous correction of VPF (VCVPF). Here we compute the pressure correction for capillary instability in cases in which one fluid is viscous and the other fluid is a gas of negligible density and viscosity. The growth rates computed using VCVPF are in remarkably good agreement with the exact solution FVF.

1. Introduction

Capillary instability of a liquid cylinder of mean radius R leading to capillary collapse can be described as a neckdown due to surface tension γ in which fluid is ejected from the neck, leading to a smaller neck and greater neckdown capillary force as seen in the diagram in figure 1.

Tomotika (1935) studied the capillary instability and gave an exact normal-mode solution of the linearized Navier–Stokes equations. This exact solution served as the standard in Funada & Joseph's (2002) analysis of capillary instability in which the flow was assumed to be irrotational. Funada & Joseph showed that the results with the viscosities of the fluids retained were in better agreement with the fully viscous flow (FVF) solution than those assuming inviscid fluids.

Joseph & Wang (2004) considered free-surface problems in which the flow is assumed to be irrotational. However, the non-zero irrotational shear stress violates the zero-shear-stress condition at the free surface. They derived a viscous correction formulation for the irrotational pressure, which is induced in a boundary layer by the uncompensated irrotational shear stress. This boundary layer is not studied and is not needed. We use this formulation to compute a pressure correction for capillary instability in cases in which one fluid is viscous and the other fluid is a gas of negligible density and viscosity.

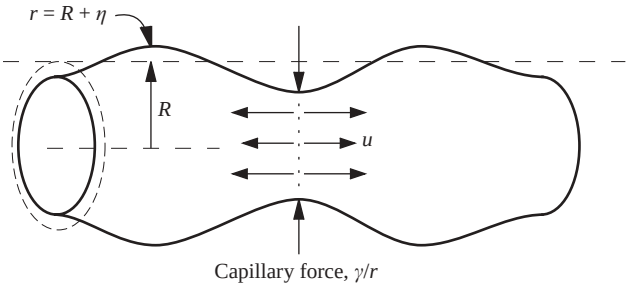

FIGURE 1. Capillary instability. The force γ/r drives fluid away from the neck, leading to collapse.

2. Linearized equations for capillary instability

Consider the stability of a liquid cylinder of radius R with viscosity μ_l and density ρ_l surrounded by another fluid with viscosity μ_a and density ρ_a under capillary forces generated by interfacial tension γ. The analysis is done in cylindrical coordinates (r, θ, z) and only axisymmetric disturbances independent of θ are considered. The linearized Navier–Stokes equations and interfacial condition are made dimensionless with the following scales:

$$[\text{length, velocity, time, pressure}] = [D,\ U,\ D/U,\ p_0]$$

where D is the diameter of the liquid cylinder, $U = \sqrt{\gamma/(\rho_l D)}$, and $p_0 = \rho_l U^2$. The three dimensionless parameters controlling the solution are $m = \mu_a/\mu_l$, $l = \rho_a/\rho_l$ and a Reynolds number $J = VD\rho_l/\mu_l = Oh^2$ where $V = \gamma/\mu_l$ and Oh is the Ohnesorge number. The governing equations are

$$\frac{\partial u_l}{\partial r} + \frac{u_l}{r} + \frac{\partial w_l}{\partial z} = 0, \tag{2.1}$$

$$\frac{\partial u_l}{\partial t} = -\frac{\partial p_l}{\partial r} + \frac{1}{\sqrt{J}}\left(\nabla^2 u_l - \frac{u_l}{r^2}\right), \quad \frac{\partial w_l}{\partial t} = -\frac{\partial p_l}{\partial z} + \frac{1}{\sqrt{J}}\nabla^2 w_l, \tag{2.2}$$

$$\frac{\partial u_a}{\partial r} + \frac{u_a}{r} + \frac{\partial w_a}{\partial z} = 0, \tag{2.3}$$

$$l\frac{\partial u_a}{\partial t} = -\frac{\partial p_a}{\partial r} + \frac{m}{\sqrt{J}}\left(\nabla^2 u_a - \frac{u_a}{r^2}\right), \quad l\frac{\partial w_a}{\partial t} = -\frac{\partial p_a}{\partial z} + \frac{m}{\sqrt{J}}\nabla^2 w_a, \tag{2.4}$$

with

$$\nabla^2 = \frac{\partial^2}{\partial r^2} + \frac{1}{r}\frac{\partial}{\partial r} + \frac{\partial^2}{\partial z^2}.$$

The kinematic condition at the interface $r = 1/2 + \eta$ (where η is the varicose displacement) is given by

$$\frac{\partial \eta}{\partial t} = u_l, \quad \frac{\partial \eta}{\partial t} = u_a. \tag{2.5}$$

The normal stress balance at the interface is given by

$$p_a - p_l + \frac{2}{\sqrt{J}}\frac{\partial u_l}{\partial r} - \frac{2m}{\sqrt{J}}\frac{\partial u_a}{\partial r} = \frac{\partial^2 \eta}{\partial z^2} + \frac{\eta}{R^2}. \tag{2.6}$$

The tangential stress balance at the interface is given by

$$\left(\frac{\partial u_l}{\partial z}+\frac{\partial w_l}{\partial r}\right)=m\left(\frac{\partial u_a}{\partial z}+\frac{\partial w_a}{\partial r}\right). \tag{2.7}$$

The continuity of the normal and tangential velocity at the interface requires respectively

$$u_l=u_a, \tag{2.8}$$

$$w_l=w_a. \tag{2.9}$$

3. Fully viscous flow (FVF) solution (Tomotika 1935)

Tomotika (1935) gave a normal-mode solution to the linearized governing equations. This is an exact solution which satisfies all the four interfacial conditions in (2.6)–(2.9). He expressed the solution with stream functions:

$$\psi_l=[A_1 r I_1(kr)+A_2 r I_1(k_l r)]\exp(\sigma t+\mathrm{i}kz), \tag{3.1}$$

$$\psi_a=[B_1 r K_1(kr)+B_2 r K_1(k_a r)]\exp(\sigma t+\mathrm{i}kz), \tag{3.2}$$

$$\eta=H\exp(\sigma t+\mathrm{i}kz), \tag{3.3}$$

where σ is the complex growth rate and k is the wavenumber; the modified Bessel functions of the first order are denoted by I_1 for the first kind and K_1 for the second kind. Substitution of (3.1)–(3.3) to (2.6)–(2.9) leads to the solvability condition, which is given as the dispersion relation:

$$\begin{vmatrix} I_1(kR) & I_1(k_lR) & K_1(kR) & K_1(k_aR) \\ kI_0(kR) & k_lI_0(k_lR) & -kK_0(kR) & -k_aK_0(k_aR) \\ 2k^2I_1(kR) & (k^2+k_l^2)I_1(k_lR) & 2mk^2K_1(kR) & m(k^2+k_a^2)K_1(k_aR) \\ F_1 & F_2 & F_3 & F_4 \end{vmatrix}=0, \tag{3.4}$$

where

$$F_1=\mathrm{i}\sigma I_0(kR)+2\mathrm{i}\frac{k^2}{\sqrt{J}}\left(\frac{\mathrm{d}I_1(kR)}{\mathrm{d}(kR)}\right)-\left(\frac{1}{R^2}-k^2\right)\mathrm{i}\frac{k}{\sigma}I_1(kR), \tag{3.5}$$

$$F_2=2\mathrm{i}\frac{kk_l}{\sqrt{J}}\left(\frac{\mathrm{d}I_1(k_lR)}{\mathrm{d}(k_lR)}\right)-\left(\frac{1}{R^2}-k^2\right)\mathrm{i}\frac{k}{\sigma}I_1(k_lR), \tag{3.6}$$

$$F_3=-\mathrm{i}l\sigma K_0(kR)+2\mathrm{i}\frac{mk^2}{\sqrt{J}}\left(\frac{\mathrm{d}K_1(kR)}{\mathrm{d}(kR)}\right),\quad F_4=2\mathrm{i}\frac{mkk_a}{\sqrt{J}}\left(\frac{\mathrm{d}K_1(k_aR)}{\mathrm{d}(k_aR)}\right), \tag{3.7}$$

with

$$k_l=\sqrt{k^2+\sqrt{J}\sigma},\quad k_a=\sqrt{k^2+\frac{l}{m}\sqrt{J}\sigma}. \tag{3.8}$$

4. Viscous potential flow (VPF) solution (Funada & Joseph 2002)

The potential flow solution is given by $\boldsymbol{u}=\nabla\phi$, $\nabla^2\phi=0$. The normal stress balance (2.6) and normal velocity continuity (2.8) are satisfied; the shear stress and tangential velocity conditions (2.7) and (2.9) cannot be enforced. The potential solution can be expressed as

$$\psi_l=A_1 r I_1(kr)\exp(\sigma t+\mathrm{i}kz), \tag{4.1}$$

$$\psi_a=B_1 r K_1(kr)\exp(\sigma t+\mathrm{i}kz), \tag{4.2}$$

$$\eta=H\exp(\sigma t+\mathrm{i}kz), \tag{4.3}$$

for which the dispersion relation is given by

$$(\alpha_l + l\alpha_a)\sigma^2 + \frac{2k^2}{\sqrt{J}}(\beta_l + m\beta_a)\sigma = \left(\frac{1}{R^2} - k^2\right)k, \tag{4.4}$$

with

$$\alpha_l = \frac{I_0(kR)}{I_1(kR)}, \quad \alpha_a = \frac{K_0(kR)}{K_1(kR)}, \quad \beta_l = \alpha_l - \frac{1}{kR}, \text{ and } \beta_a = \alpha_a + \frac{1}{kR}. \tag{4.5}$$

Solving (4.4), we obtain

$$\sigma = -\frac{k^2(\beta_l + m\beta_a)}{\sqrt{J}(\alpha_l + l\alpha_a)} \pm \sqrt{\left[\frac{k^2(\beta_l + m\beta_a)}{\sqrt{J}(\alpha_l + l\alpha_a)}\right]^2 + \left(\frac{1}{R^2} - k^2\right)\frac{k}{(\alpha_l + l\alpha_a)}}. \tag{4.6}$$

Thus instability arises in $0 < kR < 1$, for which the dimensionless critical wavenumber $k_c = 1/R = 2$. When $\sqrt{J} \to \infty$, (4.6) reduces to

$$\sigma = \pm\sqrt{\left(\frac{1}{R^2} - k^2\right)\frac{k}{(\alpha_l + l\alpha_a)}}, \tag{4.7}$$

which is just the solution in inviscid potential flow (IPF).

5. Pressure correction for VPF

We consider the case in which the exterior fluid is a gas of negligible viscosity and density, $m = l = 0$. The flow of the interior fluid is assumed to be a potential flow expressed by the stream function (4.1). The irrotational shear stress at the interface is

$$\frac{\tau_{rz}}{\gamma/D} = -\frac{2}{\sqrt{J}}A_1 k^2 I_1(kR)\exp(\sigma t + \mathrm{i}kz), \tag{5.1}$$

which violates the zero-shear-stress condition at the free surface. A pressure correction p^v induced by this discontinuity of the shear stress can be calculated. Joseph & Wang (2004) showed that the power of the pressure correction p^v is equal to the power of the irrotational shear stress

$$\int_A \tau_s u_s \,\mathrm{d}A = \int_A (-p^v)\, u_n \,\mathrm{d}A. \tag{5.2}$$

They also showed that in linearized problems, the governing equation for p^v is

$$\nabla^2 p^v = 0. \tag{5.3}$$

Solving equation (5.3), we obtain the pressure correction

$$\frac{-p^v}{\gamma/D} = \sum_{j=0}^{\infty} C_j \mathrm{i} I_0(jr)\exp(\sigma t + \mathrm{i}jz), \tag{5.4}$$

where C_j are constants. With p^v, the normal stress balance becomes

$$-p_l - p^v + \frac{2}{\sqrt{J}}\frac{\partial u_l}{\partial r} = \frac{\partial^2 \eta}{\partial z^2} + \frac{\eta}{R^2}, \tag{5.5}$$

which gives rise to

$$\left\{A_1\sigma I_0(kR)+C_kI_0(kR)+\frac{2k^2}{\sqrt{J}}A_1\left[I_0(kR)-\frac{I_1(kR)}{kR}\right]\right\}\exp(\sigma t+\mathrm{i}kz)$$
$$+\sum_{j\neq k}C_jI_0(jR)\exp(\sigma t+\mathrm{i}jz)=A_1\frac{k}{\sigma}I_1(kR)\left(\frac{1}{R^2}-k^2\right)\exp(\sigma t+\mathrm{i}kz). \quad (5.6)$$

By orthogonality of Fourier series, we obtain

$$A_1\sigma I_0(kR)+C_kI_0(kR)+\frac{2k^2}{\sqrt{J}}A_1\left[I_0(kR)-\frac{I_1(kR)}{kR}\right]=A_1\frac{k}{\sigma}I_1(kR)\left(\frac{1}{R^2}-k^2\right) \quad (5.7)$$

and $C_j=0$ if $j\neq k$. To determine the constant C_k, we use (5.2) in complex from

$$\int_A(-p^v)\bar{u}_l\,\mathrm{d}A=\int_A\tau_{rz}\bar{w}_l\,\mathrm{d}A, \quad (5.8)$$

where the overbar denotes conjugate variables. Substitution of (5.1) and (5.4) into (5.8) leads to

$$C_k=2A_1k^2/\sqrt{J}. \quad (5.9)$$

Inserting (5.9) into (5.7), we obtain the dispersion relation

$$\frac{I_0(kR)}{I_1(kR)}\sigma^2+\frac{2k^2}{\sqrt{J}}\left[\frac{2I_0(kR)}{I_1(kR)}-\frac{1}{kR}\right]\sigma=k\left(\frac{1}{R^2}-k^2\right). \quad (5.10)$$

Using the definitions in (4.5), we write (5.10) as

$$\alpha_l\sigma^2+\frac{2k^2}{\sqrt{J}}(\alpha_l+\beta_l)\sigma=k\left(\frac{1}{R^2}-k^2\right), \quad (5.11)$$

which leads to the expression for the growth rate with corrected pressure for VPF (VCVPF)

$$\sigma=-\frac{k^2(\alpha_l+\beta_l)}{\sqrt{J}\alpha_l}\pm\sqrt{\left[\frac{k^2(\alpha_l+\beta_l)}{\sqrt{J}\alpha_l}\right]^2+\left(\frac{1}{R^2}-k^2\right)\frac{k}{\alpha_l}}. \quad (5.12)$$

For the purpose of comparison, we also list the growth rates using inviscid potential flow (IPF), VPF and FVF under the condition $m=l=0$

$$\mathrm{IPF}:\sigma=\pm\sqrt{\left(\frac{1}{R^2}-k^2\right)\frac{k}{\alpha_l}}; \quad (5.13)$$

$$\mathrm{VPF}:\sigma=-\frac{k^2\beta_l}{\sqrt{J}\alpha_l}\pm\sqrt{\left[\frac{k^2\beta_l}{\sqrt{J}\alpha_l}\right]^2+\left(\frac{1}{R^2}-k^2\right)\frac{k}{\alpha_l}}; \quad (5.14)$$

FVF: σ is the solution of

$$\begin{vmatrix}2k^2I_1(kR) & \left(k^2+k_l^2\right)I_1(k_lR)\\ F_1 & F_2\end{vmatrix}=0, \quad (5.15)$$

where F_1 and F_2 are defined in (3.5) and (3.6).

We calculate the growth rate σ using IPF (5.13), VPF (5.14) and VCVPF (5.12) and compare these results with the FVF solution (5.15). We choose five fluids surrounded

Fluids	(1) Mercury–air	(2) Water–air	(3) SO100–air	(4) Glycerine–air	(5) SO10000–air
ρ_l (kg m^{-3})	1.35×10^4	1.00×10^3	9.69×10^2	1.26×10^3	9.69×10^2
μ_l (kg m^{-1} s^{-1})	1.56×10^{-3}	1.0×10^{-3}	0.1	0.782	10.0
γ (N m^{-1})	0.482	7.28×10^{-2}	2.1×10^{-2}	6.34×10^{-2}	2.1×10^{-2}
$J = \rho_l \gamma D/\mu_l^2$	2.67×10^7	7.28×10^5	20.4	1.30	2.04×10^{-3}

TABLE 1. The properties of five fluids surrounded by air used to study capillary instability and the Reynolds number $J = Oh^2$ where Oh is the Ohnesorge number.

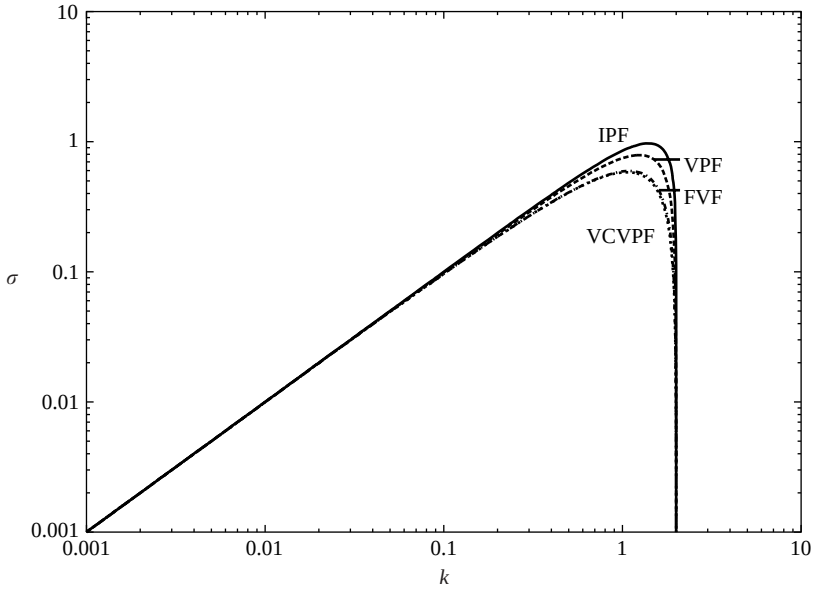

FIGURE 2. The growth rate σ vs. k for case 3, SO100 in air. IPF and VPF slightly overestimate the growth rate in the region near the peak; the curve for the corrected solution (VCPVF) is almost indistinguishable from the exact solution (FVF).

by air to study capillary instability and the properties of the fluids and Reynolds numbers are listed in table 1.

At high Reynolds numbers, the results using IPF, VPF, VCVPF and FVF are essentially the same (all the theories give rise to essentially the same result in the case of water or mercury; refer to Funada & Joseph 2002). At lower Reynolds numbers, IPF overestimates the growth rate considerably in the maximum growth region; the growth rate by VPF is in better agreement with the FVF solution; the curves for VCVPF are almost indistinguishable from the FVF curves (figure 2 and 3). The remarkably good agreement between VCVPF and FVF seems universal; it is observed for $10^{-3} < J < 10^7$ and for any $k < k_c = 2$ (see table 2).

6. Dissipation calculation for capillary instability

The same results as just obtained using a viscous correction of the inviscid pressure (VCVPF) can be obtained without such a correction by evaluating the viscous dissipation in the liquid for the irrotational flow. The dissipation method was introduced by Lamb (1932) in his study of the effect of viscosity on the decay of

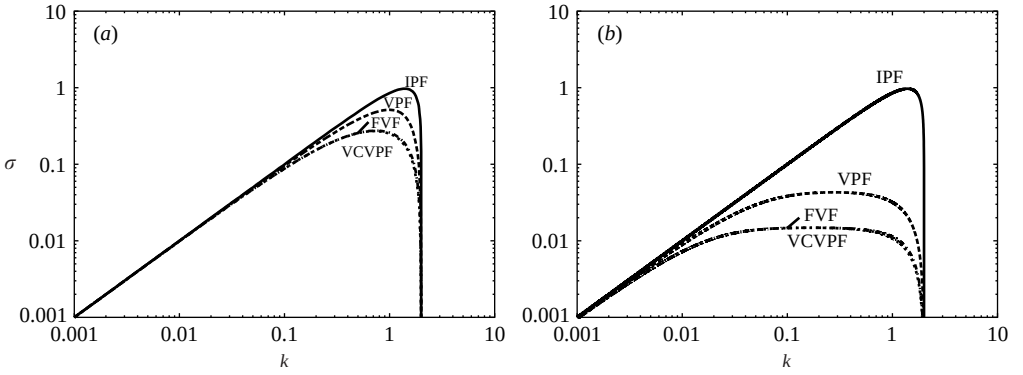

FIGURE 3. The growth rate σ vs. k for case 4, glycerine in air (*a*) and for case 5, SO10000 in air (*b*). The growth rates computed from IPF and VPF deviate considerably from the exact solution (FVF), but the growth rates from the corrected solution (VCVPF) are nearly the same as the exact solution (see table 2).

	VCVPF (A)		FVF (A)		VCVPF (B)		FVF (B)	
Case	k_m	σ_m	k_m	σ_m	k_m	σ_m	k_m	σ_m
1	1.39	0.97	1.39	0.97	0.97	2.32	0.97	2.31
2	1.39	0.97	1.39	0.97	0.96	2.31	0.96	2.31
3	1.06	0.58	1.09	0.59	0.53	1.58	0.60	1.61
4	0.72	0.27	0.74	0.28	0.21	0.84	0.28	0.86
5	0.17	0.015	0.17	0.015	0.0066	0.045	0.013	0.045

TABLE 2. Maximum growth rate σ_m and the associated wavenumber k_m for VCVPF and FVF in the five cases shown in table 1 (A) and in the five inverse cases (B) (see § 7), e.g. air–mercury.

irrotational waves on water. Here we do the dissipation calculation for the case in which the exterior fluid is a gas of negligible viscosity and density. The mechanical energy equation for the interior liquid is

$$\frac{\mathrm{d}}{\mathrm{d}t}\int_{V_l}\rho_l\frac{|\boldsymbol{u}_l|^2}{2}\mathrm{d}V=\int_A[(-p+\tau_{rr})u_l+\tau_{rz}w_l]\,\mathrm{d}A-\int_{V_l}2\mu_l\boldsymbol{D}\!:\!\boldsymbol{D}\;\mathrm{d}V. \tag{6.1}$$

The normal stress balance at the free surface gives

$$-p_l+\tau_{rr}=\gamma\left(\frac{\partial^2\eta}{\partial z^2}+\frac{\eta}{R^2}\right). \tag{6.2}$$

The shear stress at the free surface is zero:

$$\tau_{rz}=0. \tag{6.3}$$

The flow of the interior fluid is assumed to be a potential flow; the following identity can be proved easily for a potential flow:

$$\mathscr{D}=\int_V 2\mu\boldsymbol{D}\!:\!\boldsymbol{D}\,\mathrm{d}V=\int_A\boldsymbol{n}\cdot 2\mu\boldsymbol{D}\cdot\boldsymbol{u}\,\mathrm{d}A, \tag{6.4}$$

where $\mathscr{D}$ is the dissipation, A is the surface of V and $\boldsymbol{n}$ is the unit normal pointing outward. Substitution of (6.2), (6.3) and (6.4) into (6.1) gives

$$\frac{\mathrm{d}}{\mathrm{d}t}\int_{V_l}\rho_l\frac{|\boldsymbol{u}_l|^2}{2}\mathrm{d}V=\int_A\gamma\left(\frac{\partial^2\eta}{\partial z^2}+\frac{\eta}{R^2}\right)u_l\ \mathrm{d}A-\int_A\boldsymbol{n}\cdot 2\mu_l\boldsymbol{D}\cdot\boldsymbol{u}_l\ \mathrm{d}V. \tag{6.5}$$

The dimensionless form of (6.5) is

$$\frac{\mathrm{d}}{\mathrm{d}t}\int_{V_l}\frac{|\boldsymbol{u}_l|^2}{2}\mathrm{d}V=\int_A\left(\frac{\partial^2\eta}{\partial z^2}+\frac{\eta}{R^2}\right)u_l\ \mathrm{d}A-\frac{1}{\sqrt{J}}\int_A\boldsymbol{n}\cdot 2\boldsymbol{D}\cdot\boldsymbol{u}_l\ \mathrm{d}V. \tag{6.6}$$

We evaluate the integrals in (6.6) to obtain

$$\frac{\sigma+\bar{\sigma}}{2}\frac{I_0(kR)}{I_1(kR)}+\frac{2k^2}{\sqrt{J}}\left[\frac{2I_0(kR)}{I_1(kR)}-\frac{1}{kR}\right]=\frac{k}{\sigma}\left(\frac{1}{R^2}-k^2\right), \tag{6.7}$$

where the overbar indicates the complex conjugate. If we assume that σ is real, (6.7) becomes

$$\frac{I_0(kR)}{I_1(kR)}\sigma^2+\frac{2k^2}{\sqrt{J}}\left[\frac{2I_0(kR)}{I_1(kR)}-\frac{1}{kR}\right]\sigma=k\left(\frac{1}{R^2}-k^2\right), \tag{6.8}$$

which is exactly the same as the dispersion relation (5.10) from the VCVPF solution. The solution of (6.8) is

$$\sigma=-\frac{k^2(\alpha_l+\beta_l)}{\sqrt{J}\alpha_l}\pm\sqrt{\left[\frac{k^2(\alpha_l+\beta_l)}{\sqrt{J}\alpha_l}\right]^2+\left(\frac{1}{R^2}-k^2\right)\frac{k}{\alpha_l}}. \tag{6.9}$$

In the range $0\leqslant k\leqslant 1/R=2$, σ is real and our assumption is satisfied. Therefore, the growth rate by the dissipation calculation is the same as that calculated by VCVPF.

7. Cases in which the interior fluid is a gas

Next we consider cases in which the interior fluid is a gas with negligible viscosity and density; these are the inverse cases of those in § 5. We shall omit the details of the VCVPF calculation because they are similar to those presented in § 5. We directly present the growth rates computed by IPF, VPF, VCVPF and FVF as follows:

$$\mathrm{IPF}:\sigma=\pm\sqrt{\left(\frac{1}{R^2}-k^2\right)\frac{k}{\alpha_a}}; \tag{7.1}$$

$$\mathrm{VPF}:\sigma=-\frac{k^2\beta_a}{\sqrt{J'}\alpha_a}\pm\sqrt{\left[\frac{k^2\beta_a}{\sqrt{J'}\alpha_a}\right]^2+\left(\frac{1}{R^2}-k^2\right)\frac{k}{\alpha_a}}; \tag{7.2}$$

$$\mathrm{VCVPF}:\sigma=-\frac{k^2(\alpha_a+\beta_a)}{\sqrt{J'}\alpha_a}\pm\sqrt{\left[\frac{k^2(\alpha_a+\beta_a)}{\sqrt{J'}\alpha_a}\right]^2+\left(\frac{1}{R^2}-k^2\right)\frac{k}{\alpha_a}}; \tag{7.3}$$

FVF: σ is the solution of

$$\begin{vmatrix}2k^2K_1(kR) & \left(k^2+k_a'^2\right)K_1(k_a'R)\\ F_5 & F_6\end{vmatrix}=0, \tag{7.4}$$

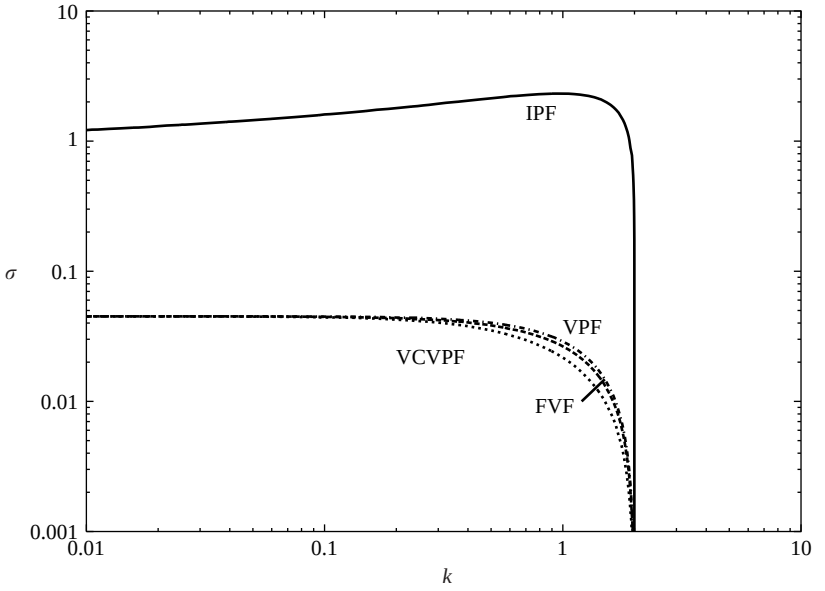

FIGURE 4. The growth rate σ vs. k for case 5 (inverse), air in SO10000. The growth rate calculated by IPF is significantly larger than that by FVF; the results by VPF, VCVPF and FVF are almost the same (see table 2).

where α_a, β_a are defined in (4.5) and

$$F_5 = -\sigma K_0(kR) - \frac{2k^2}{\sqrt{J'}}\left(\frac{\mathrm{d}K_1(kR)}{\mathrm{d}(kR)}\right) + \left(\frac{1}{R^2} - k^2\right)\frac{k}{\sigma}K_1(kR), \tag{7.5}$$

$$F_6 = -\frac{2kk'_a}{\sqrt{J'}}\left(\frac{\mathrm{d}K_1(k'_aR)}{\mathrm{d}(k'_aR)}\right) + \left(\frac{1}{R^2} - k^2\right)\frac{k}{\sigma}K_1(k'_aR), \tag{7.6}$$

with

$$k'_a = \sqrt{k^2 + \sqrt{J'}\sigma}, \quad J' = \frac{\rho_a D\gamma}{\mu_a^2}. \tag{7.7}$$

We calculate the growth rate curves for the inverse cases of those listed in table 1. Example curves are plotted in figure 4 for air in SO10000. At low Reynolds numbers (figure 4), the growth rate calculated by IPF is significantly larger than that by FVF for any $k < k_c = 2$; VPF and VCVPF both give good approximations to FVF. At higher Reynolds numbers, the growth rate curves computed using IPF, VPF, VCVPF and FVF are almost the same.

8. Discussion

The theory of the pressure correction is connected to the dissipation method. The dissipation method is based on the assumption that the velocity field in the bulk liquid is given by a potential. The dissipation method has been used in several different ways connected to the mechanical energy equation in which the dissipation integral is one term. In all the different ways that the dissipation method has been used so far no pressure, much less a pressure correction, is required; the motion of the liquid

required for implementation of the method is purely irrotational; vorticity layers are not needed or used. In the problem of the drag on a spherical gas bubble rising with the velocity U introduced by Levich (1949) and in various extensions of this problem discussed by Joseph & Wang (2004), the drag D is computed by equating the power of the rise DU to the dissipation integral evaluated on the potential flow. A dissipation calculation based entirely on irrotational theory of the decay due to viscosity of water waves given by Lamb (1932) does not involve a pressure or pressure correction. Our calculation here of growth rate curves based on the mechanical energy equation (6.5) is allied to the dissipation method; the pressure in the traction integral is eliminated in favour of the interfacial tension and the elevation function η. Using normal-mode solutions and equation (2.5), we eliminated η and expressed all the terms in (6.5) with the velocity potential.

The problems addressed by the dissipation method may also be considered by viscous potential flow (VPF), but the results are different except in special cases in which the irrotational shear stress vanishes or is very small as in the case of the rise of a spherical cap bubble (Joseph 2003), the rise of an ellipsoidal Taylor bubble (Funada *et al.* 2004) and in Rayleigh–Taylor instability (Joseph, Belanger & Beavers 1999). When the irrotational shear stress is not zero or very small, pressure corrections are induced by the discrepancy between the irrotational shear stress and the zero shear stress required by physics. The corrections cannot exist in potential flow where the pressure is determined by Bernoulli's equation. It is generally assumed that the extra pressure can be found in a vorticity boundary layer which is so small that it does not contribute to the dissipation integral. Such a theory should lead to appropriate scaling in which small terms in the governing equations could be identified, and the size of the boundary layer, the description of the distribution of velocity, vorticity and especially the distribution of the pressure could be determined. A conventional approach to the problem of the rise velocity of a spherical gas bubble, given by Moore (1963) failed to produce an acceptable pressure function for reasons identified by Kang & Leal (1988*a*) who approached the problem of the extra pressure in another way in which boundary layers are not in evidence. Regarding this approach, Kang & Leal (1988*b*) remark that "In the present analysis, we therefore use an alternative method which is equivalent to Lamb's dissipation method, in which we ignore the boundary layer and use the potential-flow solution right up to the boundary, with the effect of viscosity included by adding a viscous pressure correction and the viscous stress term to the normal stress balance, using the inviscid flow solution to estimate their values." The approach of Kang & Leal is similar to ours but its implementation, based on a rather complicated analysis of the nonlinear vorticity equation, is quite different.

Our approach to the extra pressure also does not require the analysis of a boundary layer; we have called this approach the viscous correction of viscous potential flow (VCVPF). It is based on the assumption that the motion is irrotational, the shear stress is zero, the normal stress is computed on the irrotational flow and the extra or corrected pressure can be computed at the boundary to compensate for the non-zero irrotational stress. This leads to the pressure correction formula (5.2) relating this extra pressure to the uncompensated shear stress. The extra pressure is an additional and important viscous contribution to the normal stress.

For the case of a gas bubble rising with the velocity U in a viscous fluid, it is possible to prove that the drag D_1 computed indirectly by the dissipaton method is equal to the drag D_2 computed directly by our formulation of VCVPF. Suppose that (5.2) holds and that the drag on the bubble is given as $D_1 = \mathscr{D}/U$, where $\mathscr{D}$ is the

dissipation (6.4). Then

$$D_1 = \mathscr{D}/U = \int_V 2\mu \boldsymbol{D}:\boldsymbol{D}\,\mathrm{d}V/U = \int_A \boldsymbol{n}\cdot 2\mu\boldsymbol{D}\cdot\boldsymbol{u}\,\mathrm{d}A/U$$
$$= \int_A (\tau_n u_n + \tau_s u_s)\,\mathrm{d}A/U = \int_A (-p^v + \tau_n)\,u_n\,\mathrm{d}A/U$$
$$= \int_A \boldsymbol{e}_x\cdot\boldsymbol{e}_n\left(-p^v - p^i + \tau_n\right)\mathrm{d}A = \int_A \boldsymbol{e}_x\cdot\mathbf{T}\cdot\boldsymbol{e}_n\,\mathrm{d}A = D_2, \tag{8.1}$$

where we have used the normal velocity continuity $u_n = U\boldsymbol{e}_x\cdot\boldsymbol{e}_n$, the zero-shear-stress condition at the gas–liquid interface and the fact that the irrotational pressure makes no contribution to the drag.

The VCVPF theory that we have developed for the extra pressure relies heavily on the assumption that the motion and normal stress can be computed on potential flow and the uncompensated irrotational shear stress induces an extra pressure contribution to the normal stress. For the analysis of the extra pressure we have the new pressure correction formula (5.2) and the usual equation for the pressure

$$\nabla^2 p + \rho\,\mathrm{div}\,(\boldsymbol{u}\cdot\nabla\boldsymbol{u}) = 0, \tag{8.2}$$

which reduces to $\nabla^2 p^v = 0$, even in the vorticity layer, in the linearized problem. The extra pressure p^v can be expressed on the boundary by harmonic series. In the case of the rising gas bubble, the correction formula (5.2) is enough to establish the coefficient of the principal term of the harmonic series; this term and only this term enters into the direct computation of the drag by integration of the drag component of the traction vector and this drag is the same as the one computed by the dissipation method.

For all the problems studied so far, the same results are obtained from dissipation calculations which do not involve the pressure and from direct calculations using the extra pressure p^v. This holds for the viscous decay of water waves of Lamb (1932) studied by Joseph & Wang (2004). It holds for the study of capillary instability given here. It even holds for the study of capillary instability of two viscous liquids for which the generation of internal vorticity cannot be neglected (Wang, Joseph & Funada 2004). In this problem, the zero-shear-stress interface condition is replaced by the requirement that the shear stress and tangential velocity should be continuous at the interface; neither of the two continuity conditions is satisfied in irrotational theory. Two pressure corrections are introduced here following our recipe for the construction of VCVPF. Again, we find that the dispersion relation obtained by the dissipation method and VCVPF are identical, but since internal vorticity is generated, agreement with the exact solution is not as good as in the gas–liquid case but is better than might have been expected.

Our experience with comparisons of the dissipation method and direct calculations using VCVPF suggest that fundamentally these two methods are identical. In the calculation of the drag on a gas bubble, we have already shown that the drag calculated by direct integration with a pressure correction is equal to the drag calculated by the dissipation method. However, in other problems we do not know that the results from VCVPF and the dissipation method are the same before we actually carry out the two calculations; the demonstration that the two approaches give the same results is *ex post facto*. We are not aware of a rigorous or even heuristic demonstration of equivalence of the two approaches; this question is still open.

This work was supported in part by the NSF under grants from Chemical Transport Systems.

REFERENCES

Funada, T. & Joseph, D. D. 2002 Viscous potential flow analysis of capillary instability. *Intl J. Multiphase Flow* **28**, 1459–1478.

Funada, T., Joseph, D. D., Maehara, T. & Yamashita, S. 2004 Ellipsoidal model of the rise of a Taylor bubble in a round tube. Under review.

Joseph, D. D. 2003 Rise velocity of a spherical cap bubble. *J. Fluid Mech.* **453**, 109–132.

Joseph, D. D., Belanger, J. & Beavers, G. S. 1999 Breakup of a liquid drop suddenly exposed to a high-speed airstream. *Intl J. Multiphase Flow* **25**, 1263–1303.

Joseph, D. D. & Wang, J. 2004 The dissipation approximation and viscous potential flow. *J. Fluid Mech.* **505**, 365–377.

Kang, I. S. & Leal, L. G. 1988*a* The drag coefficient for a spherical bubble in a uniform streaming flow. *Phys. Fluids* **31**, 233–237.

Kang, I. S. & Leal, L. G. 1988*b* Small-amplitude perturbations of shape for a nearly spherical bubble in an inviscid straining flow (stready shapes and oscillatory motion). *J. Fluid Mech.* **187**, 231–266.

Lamb, H. 1932 *Hydrodynamics*, 6th edn. Cambridge University Press (Reprinted by Dover 1945).

Levich, V. G. 1949 The motion of bubbles at high Reynolds numbers. *Zh. Eksp. Teor. Fiz.* **19**, 18.

Moore, D. W. 1963 The boundary layer on a spherical gas bubble. *J. Fluid Mech.* **16**, 161–176.

Tomotika, S. 1935 On the instability of a cylindrical thread of a viscous liquid surrounded by another viscous fluid. *Proc. R. Soc. Lond.* A **150**, 322–337.

Wang, J., Joseph, D. D. & Funada, T. 2004 Pressure corrections for potential flow analysis of capillary of two viscous fluids. Submitted.